Available online at www.sciencedirect.com
SCIENCE DIRECT®
Journal of Organometallic Chemistry 680 (2003) 127–135
Journal of Organometallic Chemistry
www.elsevier.com/locate/jorganchem

exo-closo-Rhodacarboranes: synthesis and characterisation of [{*exo*-$(R_3P)_2Rh$}(closo-$CB_{11}H_{12}$)] [$R_3P = P(OMe)_3$, PCy_3, 1/2dppe]

A. Rifat, V.E. Laing, G. Kociok-Köhn, M.F. Mahon, G.D. Ruggiero, A.S. Weller *

Department of Chemistry, University of Bath, Bath BA2 7AY, UK

Received 24 February 2003; received in revised form 28 March 2003; accepted 28 March 2003

Dedicated to Professor M.F. Hawthorne on the occasion of his 75th birthday

Abstract

Addition of H_2 to CH_2Cl_2 solutions of [(diene)$Rh(L)_2$][closo-$CB_{11}H_{12}$] (diene = norbornadiene, cyclooctadiene, L = PCy_3, $P(OMe)_3$, 1/2dppe) results in the formation of the *exo*-closo complexes [$(PR_3)_2$Rh(closo-$CB_{11}H_{12}$)]. These have been characterised in solution by ^{1}H- and ^{11}B-NMR spectroscopy, and for L = PCy_3 by a single crystal X-ray diffraction study. This suggests that the metal fragment is bound with the cage through the 7,8- and not the 7,12-{BH} vertices. DFT calculations on a model system where L = PMe_3 show that there is only a negligible energy difference between these two isomers (1 kcal mol^{-1}), suggesting that both represent stable structures. The salient spectroscopic markers that indicate an interaction of [closo-$CB_{11}H_{12}$]$^-$ with a metal fragment are discussed and compared across a range of metal complexes. Large upfield shifts in the ^{11}B-NMR spectrum and a small downfield shift of the CH vertex in the ^{1}H-NMR spectrum are shown to the most reliable indicators of borane interaction in solution.
© 2003 Elsevier Science B.V. All rights reserved.

Keywords: Carborane; Rhodium; NMR; Catalysis

1. Introduction

The seminal contributions made to boron chemistry by Fred Hawthorne over the last five decades have been both considerable and influential. Among these, the development of rhodacarboranes as olefin hydrogenation, isomerisation and alkenyl acetate hydrogenolysis catalysts is one of the best known. A series of papers detailing [1,2] the synthesis, structural systematics and detailed catalytic pathways of rhodacarboranes based upon [closo-{$(PPh_3)_2RhH$}$C_2B_9H_{11}$] showed that the active species in catalysis were *exo*-nido species, such as **A**. The elegant mechanism proposed (with its subsequent refinements [3]) is a striking example of where the chemistry of metallaboranes and organometallic chemistry overlap, that in order for the rhodacarborane to act as a catalyst a co-ordinately unsaturated 16-electron Rh(I) metal centre has to be formed through a 'cluster breathing' process [4] via an *exo*-nido-closo tautomerism.

More recent work by others on rhodacarboranes as olefin hydrogenation catalysts has exploited the fact that the *exo*-nido complex is the active species by tethering the metal fragment to the outside of the cage [5] and such complexes are efficient catalysts for the hydrogenation of terminal olefins (although recent reports suggest that closo compounds may also be active [6]). Recently we have adopted a different methodology to force the metal fragment *exo* to the carborane cluster, by using closo monocarborane anions, such as **B** [7], to form *exo*-closo complexes. This approach has the added advantage that, on suitable derivitisation such as perhalogenation to afford [closo-$CB_{11}H_6Br_6$]$^-$ **C**, these anions can be considered amongst the most robust and weakly coordinating known,[8] which, in turn, can result in enhanced catalytic performance. Thus [$(PPh_3)_2$Rh(closo-$CB_{11}H_{12}$)] will hydrogenate the internal alkene cyclohexene but not methylcyclohexene, but

* Corresponding author. Tel.: +44-1225-383-394; fax: +44-1225-386-231.
E-mail address: a.s.weller@bath.ac.uk (A.S. Weller).

0022-328X/03/$ - see front matter © 2003 Elsevier Science B.V. All rights reserved.
doi:10.1016/S0022-328X(03)00230-4

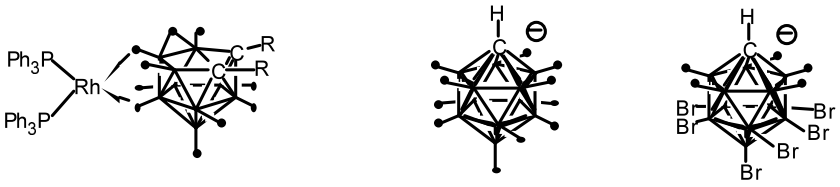

A B C

when partnered with **C** to form $[(PPh_3)_2Rh(closo\text{-}CB_{11}H_6Br_6)]_2$ the more hindered olefin can be reduced, and the catalyst is in fact active enough to reduce the sterically very hindered olefin $Me_2C{=}CMe_2$.[7] Work continues on the exact nature of the active species in these systems. As part of this, we have been investigating the synthesis of complexes of the general formula $[(R_3P)_2Rh(closo\text{-}CB_{11}H_{12})]$ where the steric and electronic influence of the phosphine is modulated. In particular we were interested in comparing, over a range of complexes, those spectroscopic markers that indicate borane interaction with the metal centre, such as the chemical shift of those {BH} vertices interacting with the metal fragment and the associated value of J(BH). We report herein the synthesis and characterisation of $[(R_3P)_2Rh(closo\text{-}CB_{11}H_{12})]$ [$R_3P = P(OMe)_3$, PCy_3, 1/2dppe].

2. Experimental

2.1. General

All manipulations were carried out under an atmosphere of argon using standard Schlenk line or glove box techniques. Solvents were dried according to standard procedures and distilled under nitrogen. NMR solvents (CD_2Cl_2, $CDCl_3$) were dried over CaH_2 for at least 24 h, vacuum distilled and freeze-pump thawed prior to use. NMR spectra were recorded on either a Bruker 300 MHz or a Varian 400 MHz spectrometer. ^{1}H-NMR spectra were referenced using residual protio solvents and ^{31}P-NMR and ^{11}B-NMR spectra were referenced to an external H_3PO_4 or $BF_3{\cdot}OEt_2$ reference, respectively. All NMR spectra were recorded at room temperature (r.t.). Coupling constants are quoted in Hz. $[(cod)Rh(closo\text{-}CB_{11}H_{12})]$ [9] and $Ag[closo\text{-}CB_{11}H_{12}]$ [10] were prepared by literature routes. All other chemicals were used as received from Strem or Aldrich.

2.2. $[(Cy_3P)_2Rh(C_7H_8)][closo\text{-}CB_{11}H_{12}]$ (**Ia**)

$[(C_7H_8)RhCl]_2$ (100 mg, 0.22 mmol) and $Ag[closo\text{-}CB_{11}H_{12}]$ (162 mg, 0.66 mmol) were placed in a Schlenk-tube and CH_2Cl_2 (25 ml) followed by 2,5-norbornadiene (0.1 ml, 0.92 mmol) were added. After 2 h the solution was filtered away from precipitated AgCl. Tricyclohexylphosphine (0.88 mmol, 248 mg) in CH_2Cl_2 (10 ml) was added to the filtrate and the solution became a deep red colour. Solvent was removed in vacuo and the product was recrystallised by dissolution in minimum CH_2Cl_2, addition of hexanes followed by cooling overnight. Yield: 150 mg (39%). *Anal.* Calc. for $C_{45}H_{88}B_{11}P_2RhCl_2$: C, 54.98; H, 8.95. Found: C, 54.7; H, 9.07%. ^{1}H-NMR (δ (ppm), $CDCl_3$): 4.63 (s, 4H, C_7H_8), 3.87 (s, 2H, C_7H_8), 3.81 (s, 2H, C_7H_8), 2.30 (s br, 1H, CH_{cage}), 1.90–1.20 (m, 77 H, C_6H_{11}, BH). $^1H\{^{11}B\}$-NMR (δ (ppm), $CDCl_3$): 4.63 (s, 4H, C_7H_8), 3.87 (s, 2H, C_7H_8), 3.81 (s, 2H, C_7H_8), 2.3 (s br, 1H, CH_{cage}), 1.9–1.2 (m, 77 H, C_6H_{11}, BH). $^{31}P\{^1H\}$-NMR (δ (ppm), $CDCl_3$): 23.6 [d, J(RhP) 145]. $^{11}B\{^1H\}$-NMR (δ (ppm), $CDCl_3$): −7.3 ppm (s, 1B), −13.6 (s, 5B), −16.4 ppm (s, 5B). ^{11}B-NMR (δ (ppm), $CDCl_3$): −7.3 [d, J(BH) 135 Hz], −13.6 [d, J(BH) 136 Hz], −16.4 [d, J(BH) 143 Hz].

2.3. $[(dppe)Rh(C_7H_8)][closo\text{-}CB_{11}H_{12}]$ (**IIa**)

$[(C_7H_8)RhCl]_2$ (97 mg, 0.21 mmol) and $Ag[closo\text{-}CB_{11}H_{12}]$ (105 mg, 0.42 mmol) were placed in a Schlenk-tube. CH_2Cl_2 and acetone (25 ml and 10 ml, respectively) were added via cannula and 2,5-norbornadiene (0.1 ml) was added via a syringe. After 2 h the solution was filtered away from precipitated AgCl. Addition of bis-diphenyl(phosphino)ethane (168 mg, 0.42 mmol) in CH_2Cl_2 (10 ml) to the filtrate resulted in the solution becoming a deep red colour. The solution was concentrated in vacuo and an equal volume of ethanol added. On cooling red, needle-like, crystals formed. Yield: 132 mg (40%). *Anal.* Calc. for $C_{35}H_{46}B_{11}Cl_2P_2Rh$: C, 51.18; H, 5.64. Found: C, 50.7; H, 5.69%. ^{1}H-NMR (δ (ppm), $CDCl_3$): 7.45 (m, 20H, C_6H_5), 5.25 (s, 4H C_7H_8), 4.20 (s, 2H C_7H_8), 2.25 [d, J(PH) 21 Hz, 4H CH_2CH_2], 2.20 (s br, 1H, CH_{cage}), 1.75 (s, 2H C_7H_8), 0.9–2.7 (q v br,

BH_{cage}). $^1H\{^{11}B\}$-NMR (δ (ppm), $CDCl_3$): 7.45 (m, 20H, C_6H_5), 5.25 (s, 4H C_7H_8), 4.20 (s, 2H C_7H_8), 2.20 [d, J(PH) 21 Hz, 4H CH_2CH_2], 2.20 (s br, 1H, CH_{cage}), 1.75 (s, 2H C_7H_8), 1.55 (s br, 6H BH), 1.39 (s br, 5H BH). $^{31}P\{^1H\}$-NMR (δ (ppm), $CDCl_3$): [d J(RhP) 156 Hz]. $^{11}B\{^1H\}$-NMR (δ (ppm), $CDCl_3$): −7.3 ppm (s, 1B), −13.6 (s, 5B), −16.4 ppm (s, 5B). ^{11}B-NMR (δ (ppm), $CDCl_3$): −7.3 [d, J(BH) 135 Hz], −13.6 [d, J(BH) 136 Hz], −16.4 [d, J(BH) 143 Hz].

2.4. [{(MeO)$_3$P}$_2$Rh(C$_8$H$_{12}$)][closo-CB$_{11}$H$_{12}$] (**IIIa**)

[(cod)Rh(closo-$CB_{11}H_{12}$)] (90 mg, 0.25 mmol) was placed in a Schlenk-tube and dissolved in CH_2Cl_2 (10 ml). $P(OMe)_3$ (63 μl, 0.50 mmol) was added dropwise via a syringe. The solution was stirred for 1 h after which the solvent was removed in vacuo. Yield: 130 mg (87%). *Anal.* Calc. for $C_{15}H_{42}B_{11}O_6P_2Rh$: C, 29.91; H, 7.03. Found: C, 30.9; H, 6.74%. ^{1}H-NMR (δ (ppm), CD_2Cl_2): 5.58 (s, 4H, CH), 3.65 (m, 18H, OCH_3), 2.50 (m, 4H, C_8H_{12}), 2.30 (m, 4H, C_8H_{12}), 2.21 (s, br, CH_{cage}), 1.50 (q br, 11H, BH). $^1H\{^{11}B\}$-NMR (δ (ppm), CD_2Cl_2): δ 5.58 (s, 4H, C_8H_{12}), 3.65 (m, 18H, OCH_3), 2.50 (m, 4H, C_8H_{12}), 2.30 (m, 4H, C_8H_{12}), 2.21 (s, br, CH_{cage}), 1.55 (s br, 6H, BH), 1.39 (s br, 5H, BH). $^{31}P\{^1H\}$-NMR (δ (ppm), CD_2Cl_2): 121 [d, J(RhP) (278 Hz)]. $^{11}B\{^1H\}$-NMR (δ (ppm), $CDCl_3$): −7.3 ppm (s, 1B), −13.6 (s, 5B), −16.4 ppm (s, 5B). ^{11}B-NMR (δ (ppm), $CDCl_3$): −7.3 [d, J(BH) 135 Hz], −13.6 [d, J(BH) 136 Hz], −16.4 [d, J(BH) 143 Hz].

2.5. [(Cy$_3$P)$_2$Rh(closo-CB$_{11}$H$_{12}$)] (**Ib**)

Compound (**Ia**) (50 mg, 0.056 mmol) was dissolved in 5 ml CH_2Cl_2 in a Young's tube. The solution was freeze-pump degassed three times. On the final cycle the tube was sealed at liquid N_2 temperatures under an atmosphere of H_2. The solution was allowed to warm to r.t. and stirred for 0.5 h. A red powder was obtained via addition of hexanes and subsequent removal of solvents in vacuo. Single crystals suitable for an X-ray diffraction study were grown by slow evaporation of a CH_2Cl_2 solution under a flow of argon. Yield: 34 mg (76%). *Anal.* Calc. for $C_{37}H_{78}B_{11}P_2Rh$: C, 55.08; H, 9.74. Found: C, 56.9; H, 10.1%. ^{1}H-NMR (δ (ppm), $CDCl_3$): 2.50 (s br, 1H, CH_{cage}), 2.00–1.00 (m br, 66H+5H, C_6H_{11} and BH), −0.62 (q br, 5H BH), −2.32 [q br, J(BH) 130, 1H BH]. $^1H\{^{11}B\}$-NMR (δ (ppm), $CDCl_3$): 2.50 (s br, 1H, CH_{cage}), 2.00−1.00 (m br, 66H+5H, C_6H_{11} and BH), −0.62 (s br, 5H BH), −2.32 (s br, 1H BH). $^{31}P\{^1H\}$ (δ (ppm), $CDCl_3$): 56.7 [d, J(RhP) 190 Hz]. ^{11}B-NMR (δ (ppm), $CDCl_3$): −11.2 [d, 1B J(BH) 130 Hz], −16.7 (br s, 5+5B coincidence). $^{11}B\{^1H\}$-NMR (δ (ppm), $CDCl_3$): −11.2 (s 1B), −16.7 (br s, 10B).

2.6. [{(MeO)$_3$P}$_2$Rh(closo-CB$_{11}$H$_{12}$)] (**IIb**)

Compound (**IIa**) (55 mg, 0.038 mmol) was dissolved in 5 ml CH_2Cl_2 in a Young's tube. The solution was freeze-pump degassed three times. On the final cycle the tube was sealed at liquid N_2 temperatures under an atmosphere of H_2. The solution was allowed to warm to r.t. and stirred for 1.5 h. Concentration of the solution in vacuo and addition of hexanes yielded a bright yellow powder. Yield: 37 mg (74%). *Anal.* Calc. for $C_7H_{30}B_{11}O_6P_2Rh$: C, 15.17; H, 5.46. Found: C, 15.8; H, 5.72%. ^{1}H-NMR (δ (ppm), CD_2Cl_2): 3.55 (m, 18H, CH_3O), 2.56 (s br, 1H, CH_{cage}), 1.81 (v br q, 5H, BH), 0.22 (v br q, 5H, BH), −2.45 [q br, J(BH) 120 Hz, 1H, BH]. $^1H\{^{11}B\}$-NMR: (δ (ppm), CD_2Cl_2): 3.55 (m, 18H, CH_3O), 2.55 (s br, 1H, CH_{cage}), 1.85 (br s, 5H, BH), 0.23 (s br, 5H, BH), −2.45 [s br, 1H, BH]. $^{31}P\{^1H\}$-NMR (δ (ppm), CD_2Cl_2): 126 [d, J(RhP) 294 Hz]. ^{11}B $\{^1H\}$-NMR (δ (ppm), CD_2Cl_2): −15.0 (shoulder, 1B) −16.0 (br s, 5+5 coninicidence). ^{11}B-NMR (δ (ppm), CD_2Cl_2): −16.0 [d, J(BH) 131 Hz].

2.7. [(dppe)Rh(closo-CB$_{11}$H$_{12}$)] (**IIIb**)

Compound (**IIIa**) (50 mg, 0.0678 mmol) was dissolved in 5 ml CH_2Cl_2 in a Young's tube. The solution was freeze-pump thawed three times. On the final cycle the tube was sealed at liquid N_2 temperatures under an atmosphere of H_2. The solution was allowed to warm to r.t. and stirred for 0.5 h. Upon addition of hexane and removal of the solvents in vacuo a peach coloured powder was obtained. Recrystallisation was achieved by slow diffusion of pentane into a CH_2Cl_2 solution of the compound. Yield: 24 mg (62%). *Anal.* Calc. for $C_{27}H_{36}B_{11}P_2Rh$: C, 50.33%; H, 5.63%. Found: C, 50.8%; H, 4.94%. ^{1}H-NMR (δ (ppm), CD_2Cl_2): 7.50 (m, 20H, C_6H_5), 2.55 (s br, 1H, CH_{cage}), 2.13 [dd, J(PH) 21 Hz, ^3J(PH) 1.6 Hz, 4H, CH_2CH_2], 1.80 (q br, 5H BH), 0.41 (q br, 5H, BH), −1.40 [q br, J(BH) 116 Hz, 1H, BH]. $^1H\{^{11}B\}$-NMR (δ (ppm), CD_2Cl_2): 7.50 (m, 20H, C_6H_5), 2.55 (s br, 1H, CH_{cage}), 2.13 [dd, J(PH) 21 Hz, ^3J(PH) 1.6 Hz, 4H, CH_2CH_2], 1.80 (s br, 5H, BH), 0.41 (s br, 5H, BH), −1.40 (s br, 1H, BH). ^{31}P-NMR (δ (ppm), CD_2Cl_2): 80.3 [d, J(RhP) 189 Hz]. $^{11}B\{^1H\}$-NMR (δ (ppm), CD_2Cl_2): −7.1 (s)*, −13.1 (s)*, −15.8 (s). ^{11}B-NMR (δ (ppm), CD_2Cl_2): −7.1 [d]*, −12.5 [d]*, −15.8 [d, 5+5+1 coincidence, J(BH) 121 Hz].[1]

2.8. X-ray crystallography

The crystal structure data for compound **Ib** were collected on a Nonius κCCD diffractometer. Structure

[1] * Assigned to uncoordinated [closo-$CB_{11}H_{12}$]$^-$ in [{$Ph_2PCH_2CH_2PPh(\eta^6$-$C_6H_5)$}Rh]$_2$[closo-$CB_{11}H_{12}$]$_2$, see text.

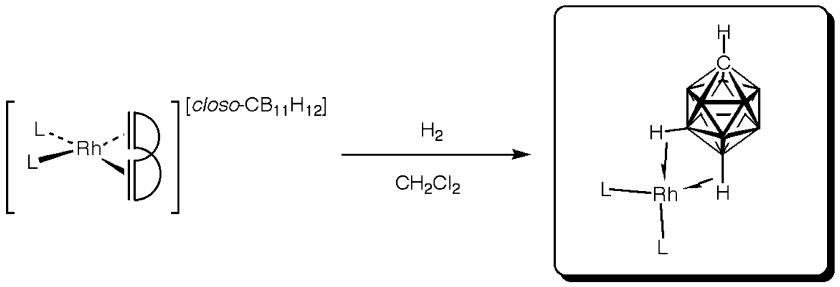

L	
Cy_3	**1**
$P(OMe)_3$	**Ia**
$P(OMe)_3$	**IIa**
$^1/_2$ dppe	**IIIa**

L	
PPh_3	**1**
PCy_3	**Ib**
$P(OMe)_3$	**IIb**
$^1/_2$ dppe	**IIIb**

Scheme 1.

solution, followed by full-matrix least-squares refinement was performed using the SHELX suite of programs throughout [11]. Two cyclohexyl groups (based on C26 and C31) are disordered over two sites in an occupancy ratio of 57:43. The location of carbon vertices {CH} in carborane cages can be problematic, given the single electron difference between boron and carbon. For complex **Ib** a number of crystallographic indicators were used to identify the most probable location of the {CH} vertex: (i) The bond distances to C(1) are consistently smaller than other bond distances in the cage (average 1.725 vs. 1.767 Å). (ii) Replacement of all the cage heteroatoms as carbons and freely refining the site occupancy resulted in C(1) having the highest occupation factor (0.93) while the others were significantly lower (0.75–0.81). (iii) wR_2 reduces slightly, but significantly, only when this vertex is assigned to carbon. Other possible isomers resulted in an increase in the weighted R factor. For this reason we are reasonably confident about the location of the carbon vertex and thus the coordination mode (7,8) of the metal fragment with respect to the cage. All hydrogen atoms were included at calculated positions.

2.9. DFT calculations

Gas-phase geometry optimisation for all multi-nuclear solutes were performed using the GAMESS-UK program using DFT at the B3LYP hybrid [12] method with the DZVP basis sets [13]. Geometry optimisation for minima used the Berny routine [14], whilst the nature of each stationary point was verified through frequency calculations. The starting point of the geometry optimisations were derived from the X-ray structure, with the six cyclohexyl groups substituted with methyl. The final absolute energies for the 7,8 and 7,12 isomers are −5928.84534 Hartrees (7,12-isomer) and −5928.84386 Hartrees (7,8-isomer), equivalent to a 0.93 kcal mol^{-1} difference in favour of the 7,12-isomer. The energies of the 2,3 and 2,7-isomers were −5298.83556 and −5928.83456 Hartrees, respectively. Coordinates of refined structures are available on request from the authors (1 Hartee = 627.5095 kcal mol^{-1}).

3. Results

We have chosen to approach the synthesis of compounds of the general formula $[L_2Rh(closo\text{-}CB_{11}H_{12})]$ by reductive hydrogenation [15] of precursor diene {1,5-cyclooctadiene (cod) or norbornadiene (nbd)} rhodium-phosphine cations partnered with $[closo\text{-}CB_{11}H_{12}]$. For $L = PCy_3$ or dppe we have synthesised new complexes $[L_2Rh(diene)][closo\text{-}CB_{11}H_{12}]$ ($L = PCy_3$, **Ia**; 1/2dppe, **IIIa**) by sequential addition of $Ag[closo\text{-}CB_{11}H_{12}]$ and phosphine to $[(nbd)RhCl]_2$. For $L = P(OMe)_3$ addition of phosphite to $[(cod)Rh(closo\text{-}CB_{11}H_{12})]$ [9] afforded $[\{P(OMe)_3\}_2Rh(cod)][closo\text{-}CB_{11}H_{12}]$ (**IIa**) by displacement of the anion. All these complexes display ^{1}H-, $^{31}P\{^1H\}$- and ^{11}B-NMR spectra that are in full accord with their formulation. All three compounds show ^{11}B spectra assigned to 'free' (i.e. not metal bound [16]) $[closo\text{-}CB_{11}H_{12}]^-$ by three doublet resonances in the ratio 1:5:5 centred at δ −7.3, −13.6 and −16.4 ppm, assigned to B(12), B(7–11) and B(2–6), respectively. In the ^{1}H-NMR spectra the cage CH resonances are all observed at ca. δ 2.20 ppm. The $^{31}P\{^1H\}$-NMR spectra of all three complexes show a single phosphorus environment displaying ^{103}Rh–^{31}P coupling. Treatment of stirred CH_2Cl_2 solutions of **Ia** to **IIIa** with H_2 resulted in reduction of the diene (as observed by ^{1}H-NMR spectroscopy in CD_2Cl_2 solution) and coordination of the $[closo\text{-}CB_{11}H_{12}]^-$ anion to the rhodium as shown by ^{1}H-, ^{11}B-, ^{31}P-NMR spectroscopy and for $L = PCy_3$ by single crystal X-ray diffraction (Scheme 1).

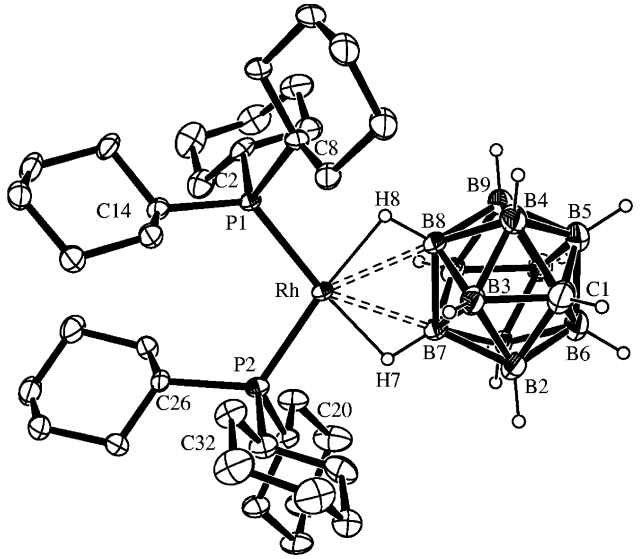

Fig. 1. Molecular structure of **Ib** showing the atom-labelling scheme. Ellipsoids are drawn at the 30% probability level. Two cyclohexyl groups [C(26) and C(32)] are disordered, with the major (57%) component shown. Cyclohexyl group hydrogen atoms have been omitted for clarity.

The molecular structure of $[(PCy_3)_2Rh(closo\text{-}CB_{11}H_{12})]$ (**Ib**) is shown in Fig. 1 with relevant data given in Tables 1 and 2. The molecule crystallises with no close intermolecular contacts in the solid state. The

Table 1
Crystal data and structure refinement for **Ia**

Empirical formula	$C_{37}H_{78}B_{11}P_2Rh$
Formula weight	806.75
Temperature (K)	150(2)
Wavelength (Å)	0.71073
Crystal system	Monoclinic
Space group	$P2_1/c$
Unit cell dimensions	
a (Å)	13.4890(5)
b (Å)	15.7790(7)
c (Å)	20.8540(9)
α (°)	90
β (°)	90.239(2)
γ (°)	90
V (Å^3)	4438.6(3)
Z	4
D_{calc} (Mg m^{-3})	1.207
Absorption coefficient (mm^{-1})	0.483
$F(000)$	1720
Crystal size (mm^3)	0.25 × 0.15 × 0.15
θ Range for data collection (°)	3.82–24.18
Reflections collected	15825
Independent reflections	6683 [$R_{int} = 0.0577$]
Reflections observed ($>2\sigma$)	5118
Refinement method	Full-matrix least-squares on F^2
Data/restraints/parameters	6683/0/564
Goodness-of-fit on F^2	1.048
Final R indices [$I > 2\sigma(I)$]	$R_1 = 0.0462$, $wR_2 = 0.0962$
R indices (all data)	$R_1 = 0.0682$, $wR_2 = 0.1061$
Largest difference peak and hole (e Å^{-3})	0.689 and −0.357

Table 2
Bond lengths (Å) and bodn angles (°) for **Ib**

Bond lengths			
Rh–P(1)	2.2770(10)	Rh–P(2)	2.2630(11)
Rh–B(8)	2.389(5)	Rh–B(7)	2.393(5)
C(1)–B(6)	1.707(9)	C(1)–B(2)	1.738(7)
C(1)–B(3)	1.710(7)	C(1)–B(4)	1.742(8)
C(1)–B(5)	1.727(10)	C(1)–B(5)	1.732(10)
B(1)–B(2)	1.772(9)	B(1)–B(5)	1.752(9)
B(1)–B(6)	1.739(9)	B(2)–B(3)	1.722(10)
B(2)–B(7)	1.738(10)	B(2)–B(8)	1.743(9)
B(3)–B(9)	1.763(8)	B(3)–B(8)	1.783(10)
B(3)–B(4)	1.795(8)	B(4)–B(5)	1.770(9)
B(4)–B(10)	1.769(9)	B(4)–B(9)	1.779(8)
B(5)–B(10)	1.765(8)	B(5)–B(6)	1.776(10)
B(6)–B(7)	1.787(8)	B(6)–B(10)	1.784(8)
B(6)–B(11)	1.804(8)	B(7)–B(8)	1.771(9)
B(7)–B(11)	1.767(8)	B(8)–B(9)	1.770(8)
Bond angles			
P(2)–Rh(1)–B(8)	147.46(12)	P(1)–Rh(1)–B(8)	105.62(12)
P(2)–Rh(1)–B(7)	105.61(13)	P(1)–Rh(1)–B(7)	147.79(13)
P(2)–Rh(1)–P(3)	106.55(4)	B(8)–Rh(1)–B(7)	42.24(16)

Rh(I) centre is square planar coordinated by the two PCy_3 ligands and two {HB} vertices [dihedral angle P(1)–P(2)–B(7)–B(8) = 5.6°]. The Rh–P bonds lengths [2.2770(10) and 2.2630(11) Å] are slightly longer than those observed in [*cis*-$\{PCy_3\}_2$(acac)Rh] [2.252(1), 2.260(1) Å] [17] but shorter than those found in [trans–$(MeCN)_2Rh\{PCy_3\}_2][BF_4]$ [2.342(2), 2.340(2) Å] [18]. The P(2)–Rh(1)–P(1) angle in **Ib** [106.55(4)°] is also comparable to the (acac) adduct [105.63(4)°]. The Rh(1)–B distances in **Ib** [Rh(1)–B(7) 2.393(5) Å and Rh(1)–B(8) 2.389(5) Å] are essentially similar to those observed in $[(PPh_3)_2Rh(closo\text{-}CB_{11}H_{12})]$ (1) [7] and $[(cod)Rh(closo\text{-}CB_{11}H_{12})]$ [9]. The cage carbon vertex has been located (see experimental), making the $\{(PCy_3)_2Rh\}^+$ fragment bind with the B(7) and B(8) lower pentagonal belt vertices of the cage anion, which contrasts with all of the crystallographically characterised monometallic transition metal complexes in which either B(12) coordination (monodentate) or B(12)/B(7) (bidentate) is suggested [7,9,19–21]. The caveat for the placement of {CH} vertices in carboranes is that they are often difficult to distinguish from {BH}, given the one electron difference between the two, and consequently their absolute position must sometimes be treated with caution. Given the degree of uncertainty regarding the {CH} placement in the solid-state, and the unusual, but tentative, 7,8-coordination mode we decided to briefly investigate the energies of the four possible isomers (7,12, 7,8, 2,7 and 2,3) by DFT methods using $[(PMe_3)_2Rh(closo\text{-}CB_{11}H_{12})]$ as a model system. The calculated structures for the 7,12 and 7,8-isomers are shown in Fig. 2.

At the B3LYP/DZVP level there is only a small energy difference (1 kcal mol^{-1}) between the 7,12-

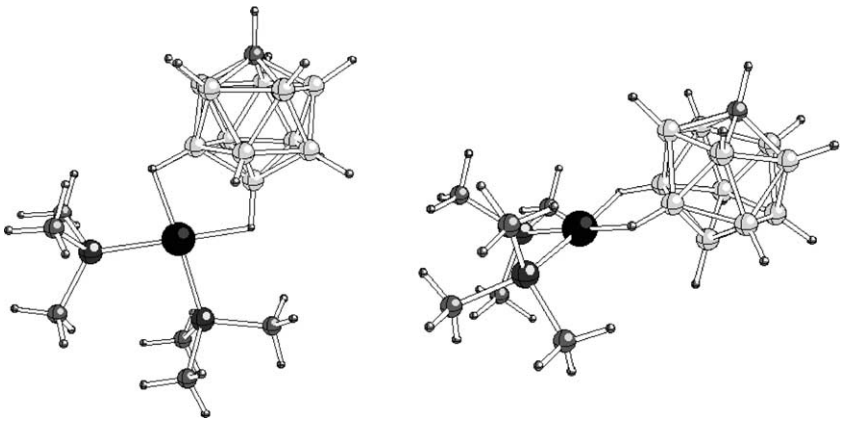

Fig. 2. DFT optimised structures of 7,12-isomer (left) and 7,8-isomer (right) of complex **Ib** (with Me substituted for Cy). The 7,12-isomer is ca. 1 kcal mol^{-1} lower in energy.

isomer and the 7,8-isomer, the former slightly favoured, and both are significantly more stable (ca. 6 kcal mol^{-1}) than the 2,3 and 2,7 isomers. This is in accordance with the observation that the B(12) vertex is the first to undergo electrophilic substitution (i.e. it is the most basic), with the lower pentagonal belt vertices next [22,23], and thus might be expected to interact with the metal fragment more strongly. That this energy difference between 7,12- and 7,8- isomers is essentially negligible suggests that both could be equally favoured at room temperature in the solid-state or solution, ignoring any solid-state (i.e. crystal packing) effects. Although this does not particularly aid in the definitive assignment of the carbon vertex in the X-ray structure of **Ib**, the small energy difference does indicate that 7,12 binding of a metal fragment is not unequivocal and that other isomeric forms are perfectly reasonable energetically, and the assignment of **Ib** as the 7,8-isomer is plausible. We have not calculated the structure or energy of any potential transition state between the two isomers, but given that both the 7- and 12-isomers are present in solution for $[Cp(CO)_2Fe(closo\text{-}CB_{11}H_{12})]$ [23] and $[Cp(CO)_3Mo(closo\text{-}CB_{11}H_{12})]$ [24] and in dynamic equilibrium with each other at room temperature, while $\{L_2M\}^+$ (M = Rh, Pt) [7,20] and $\{PPh_3Ag\}^+$ [25] fragments are all fluxional over the lower polyhedral surface of the cage even at low temperature, the energy barrier between isomers must be relatively small.

In solution the $\{(PCy_3)_2Rh\}^+$ fragment is interacting with the carborane cage and is fluxional over the lower polyhedral surface [B(7)–B(12)] of the cage. We [7,9,16,24,25] and others [19,20], have previously experimentally observed such dynamic behaviour with various metal fragments partnered with $[closo\text{-}CB_{11}H_{12}]^-$. In the $^1H\{^{11}B\}$-NMR spectrum, complex **Ib** shows upfield shifted resonances assigned to BH(7–11) [δ −0.62 ppm, 5H] and BH(12) [δ −2.32 ppm, 1H], compared with **Ia** in which the anion is not interacting. The latter resonance becomes a well defined broad quartet [J(BH) 130 Hz] in the ^1H-NMR spectrum. The $^{11}B\{^1H\}$-NMR spectrum displays two resonances, at δ −11.2 (1 B) and −16.7 (10 B) ppm, which are assigned to B(12) and coincident B(7–11) and B(2–6), respectively, with B(12) and B(7–11) shifted significantly upfield compared with **Ia** on metal coordination. The integral 1-boron resonance becomes a well defined doublet in the ^{11}B-NMR spectrum [J(HB) 130 Hz] mirroring the value observed in the ^1H-NMR spectrum. This ^1H–^{11}B coupling constant is only slightly reduced from that observed for uncoordinated $[closo\text{-}CB_{11}H_{12}]$ [135 Hz]. Overall this data shows that, on the NMR timescale, the metal fragment interacts with the unique antipodal {BH} vertex and all the lower pentagonal belt vertices. The dynamic behaviour of the rhodium fragment over the lower polyhedral surface of the cage is also shown by a single phosphorus environment being observed in the $^{31}P\{^1H\}$-NMR spectrum, even at low (−70 °C) temperature. A mechanism to account for the fluxionality has been suggested, that involves the metal fragment staying attached with B(12) and processing around the lower polyhedral faces [9,20]. However, given the small difference in energy between the 7,12 and 7,8 isomers as calculated by DFT we now suggest a modified mechanism that invokes the $\{(R_3P)_2Rh\}^+$ fragment 'walking' over the lower polyhedral surface (Scheme 2) in a 7,12⇔7,8⇔8,12 processes. In fact this mechanism is very similar to that originally proposed by Hawthorne for the fluxional behaviour of [*exo*-$\{(PPh_3)_2Rh\}$-nido-$Me_2C_2B_9H_{10}$] [2].

Treatment of **IIa** with H_2 in CH_2Cl_2 affords a pale yellow product in good yield, formulated as $[\{P(OMe)_3\}_2Rh(closo\text{-}CB_{11}H_{12})]$ (**IIb**). Despite repeated attempts crystals suitable for X-ray diffraction where not forthcoming. Never-the-less spectroscopic data unambiguously identify **IIb** has having a $\{Rh(P(OMe)_3)_2\}^+$ fragment *exo*-polyhedrally coordinated to the lower surface of the cage anion. Similar to **Ib**, upfield shifted signals are observed in the ^{11}B- and ^1H-

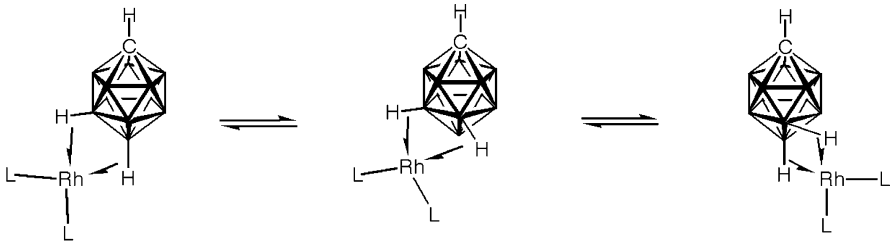

Scheme 2.

NMR spectra for those vertices that are interacting with the metal. Notably, in the ^{1}H-NMR spectrum, the antipodal {BH} vertex is observed at δ −2.45 ppm with a reduced ^{1}H–^{11}B coupling constant [J(120) Hz], while in the ^{11}B-NMR spectrum two resonances due to almost coincident 1+10 signals are observed at −15.0 and −16.0, respectively, the former a shoulder on the larger resonance. Like **Ib** signals due to B(12) and B(7–11) {BH} vertices are shifted on metal coordination. Fig. 3a presents the ^{1}H{^{11}B}-NMR spectrum of **IIb** immediately after treatment of **IIa** with H_2 in CD_2Cl_2 solution, showing the characteristic chemical shift pattern (5:5:1 low field to high field) for [closo-$CB_{11}H_{12}$] coordinated with a $\{L_2Rh\}^+$ fragment. Fig. 3b compares the ^{11}B{^{1}H}-NMR spectra of **IIa** and **IIb**, showing the upfield shift on coordination. A single resonance is observed in the ^{31}P{^{1}H}-NMR spectrum showing coupling to ^{103}Rh.

Addition of H_2 to [(dppe)Rh(nbd)] (**IIIa**) affords the new complex [(dppe)Rh(closo-$CB_{11}H_{12}$)] (**IIIb**). ^{1}H and ^{11}B-NMR spectroscopy shows that, in solution, the $\{(dppe)Rh\}^+$ fragment coordinates to the antipodal {BH} vertex and is fluxional over the lower pentagonal belt {BH} vertices. Thus, the characteristic three resonances in the ^{1}H-NMR spectrum centred at δ −1.40 (1H), 0.41 (5H), 1.80 ppm (5H) are assigned to antipodal, lower and upper pentagonal belt {BH} vertices respectively. The unique {BH} vertex shows a reduced J(BH) coupling constant of 116 Hz. In the ^{11}B-NMR spectrum of **IIIb**, a signal major peak is observed at δ −15.8 ppm. However, unlike **Ib** and **IIb**, there was always a small amount (ca. 5%) uncoordinated [closo-$CB_{11}H_{12}]^-$ observed in solution [δ^{11}B: 1:5:5 at δ −7.3, −13.6 and −16.4 ppm]. Close inspection of the ^{1}H-NMR spectrum also shows the presence of a minor component in solution by resonances between δ 7.5 and 5.5 ppm, which are diagnostic of arene coordination to a metal fragment. Moreover, the ^{31}P{^{1}H}-NMR spectrum shows a major component at δ 80.3 ppm which we assign to **IIIb**, and two much smaller multiplets at δ 81.4 and 79.4 ppm which are very similar to those reported by Fairlie and Bosnich [26] for the arene bridged dimer [{$Ph_2PCH_2CH_2PPh(\eta^6$-$C_6H_5)$}$Rh]_2[ClO_4]_2$, which has been crystallography characterised by Halpern et al. [27]. We thus assign the minor component as the dimeric complex [{$Ph_2PCH_2CH_2PPh(\eta^6$-$C_6H_5)$}$Rh]_2$[closo-$CB_{11}H_{12}]_2$. We have previously observed a similar arene bridged dimer when using the weakly coordinating anion [closo-$CB_{11}H_6Br_6]^-$, in which this anion is a poorer ligand than the phosphine aryl group [7]. In contrast the [closo-$CB_{11}H_{12}$] anion is actually quite a good ligand, for example in [$(PPh_3)_2$Rh(closo-

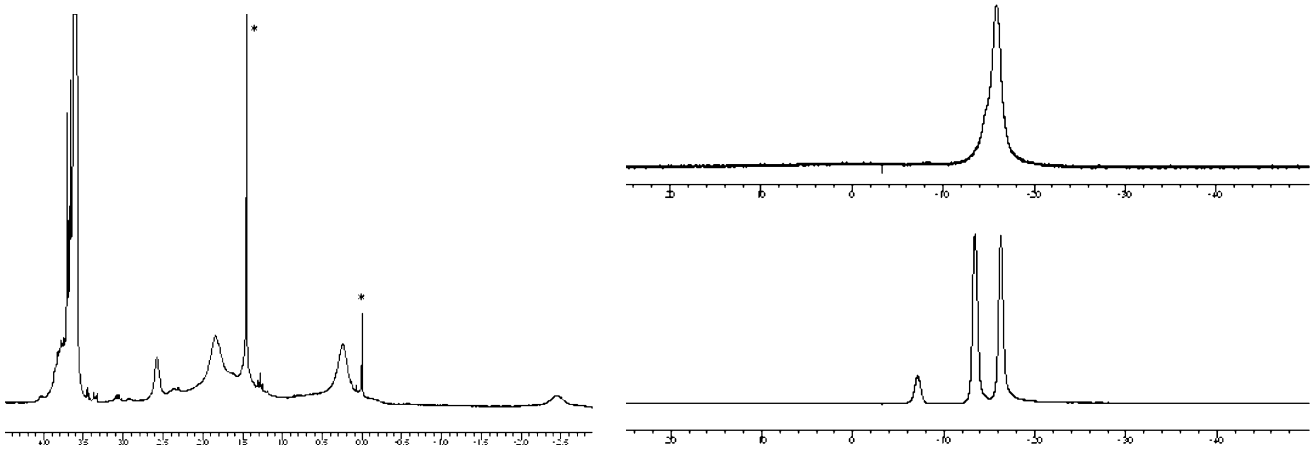

Fig. 3. (a) ^{1}H{^{11}B}-NMR spectrum of **IIb** generated in situ from **IIa** and H_2. Asterisks indicate cyclooctane and grease respectively. (b) ^{11}B{^{1}H}-NMR spectra of **IIb** (top) and **IIa** (bottom) in CD_2Cl_2.

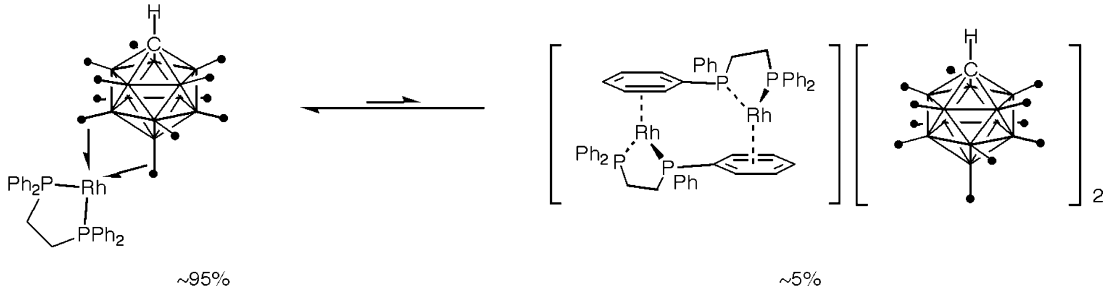

Scheme 3.

$CB_{11}H_{12}$)]. Steric factors must thus be operating to force the cage off the metal centre. We suggest that the constrained bite angle of the dppe ligand results in unfavourable interactions between the phenyl groups and anion resulting in a small amount of the dimer to be formed in solution (Scheme 3).

4. Discussion

Coordination of an $\{L_2Rh\}^+$ fragment with [closo-$CB_{11}H_{12}$] results in a characteristic upfield shift of those {BH} vertices involved in interaction with the d^8-metal fragment and a general reduction of J(HB), with the antipodal vertex most shifted. Thus, B(12) and B(7–11) shift upfield, while B(2–6) stay essentially the same. This is consistent with the fact that the ^{11}B chemical shift of a {BH} vertex is sensitive to both electron density and its orbital characteristics, both of which are expected to change significantly on metal coordination [28]. The salient spectroscopic data for the five examples we have now synthesised [PPh_3 [7], PCy_3, $P(OMe)_3$, dppe and cod [9]] as well as other metal complexes of [closo-$CB_{11}H_{12}]^-$ are compared in Table 3. The majority of these complexes show a high-field quartet in the ^{1}H-NMR spectrum assigned to the antipodal {BH} vertex and a concomitant reduction of J(BH). However there is no clear relationship between these two spectroscopic markers. For example, **Ib** has the largest coupling constant [J(BH) 130 Hz] (implying the weakest M–H–B bond) but a chemical shift [δ −2.32 ppm] that is more hydridic than the complex with the smallest coupling constant (**IIb**) [116 Hz and δ −1.40 ppm]. The ^{11}B chemical shift change ($\Delta\delta$ ^{11}B) on coordination always shows an a large upfield shift of B(12) with a smaller shift for B(7–11) and virtually no change for B(2–6) [16], but magnitude of this shift does not always correlate with J(HB), neither does it with the ^{1}H chemical shift. For example [(PPh_3)Ag(closo-$CB_{11}H_{12}$)] shows the characteristic ^{11}B chemical shift changes but no highfield ^{1}H-NMR signals due to Ag–H–B bonds. In contrast [$Cp(CO)_3Mo$(closo-$CB_{11}H_{12}$)] has a very high field chemical shift (δ −15 ppm) for the unique bridging hydride and low J(BH) [87 Hz] but the ^{11}B-NMR spectrum is not significantly different from any other with coordinated [closo-$CB_{11}H_{12}$]. Interestingly, although it is somewhat remote from those polyhedral faces involved in metal coordination, for every example reported, coordination of the metal fragment results in a (albeit small) downfield shift of the cage CH proton by

Table 3
Comparison of chemical shifts and coupling constant data for the new compounds **I** to **III** with other complexes of [closo-$CB_{11}H_{12}]^-$

	δ (^{1}H) CH (ppm) [a]	J(RhP) (Hz) [b]	δ (^{1}H) BH (ppm) [c]	J(BH) (Hz)	$\Delta\delta$ (^{11}B) (ppm) [d]		
					B(12)	B(7–11)	B(2–6)
{$(PCy_3)_2Rh$} (**Ib**)	2.50	190 (145)	*−2.32*, −0.62 [e]	130	−6.1	−3.1	0.3
{(dppe)Rh} (**IIb**)	2.55	189 (156)	*−1.40*, 0.41, 1.80	116	−8.4	−2.1	−0.7
{$(P(OMe)_3)_2Rh$} (**IIIb**)	2.55	294 (278)	*−2.45*, 0.23, 1.85	120	−7.7	−2.4	−0.4
{$(PPh_3)_2Rh$} (**1**)	2.60	194 (154)	*−1.97*, −0.70, 1.70	119	−5.7	−2.9	0.7
{(cod)Rh}	2.61	–	*−3.92*, 0.06, 1.86	109	−8.9	−1.9	−0.2
$\{Cp(CO)_3Mo\}^+$	2.53	–	*−15.11*, 1.79, 1.66	87	−6.2	−1.2	0.6
$\{(PPh_3)Ag\}^+$	2.59	–	*2.34*, 1.94, 1.76	118	−6.1	−0.7	−1.3
$\{(PPh_3)_2Ag\}^+$	2.21	–	*2.21*, 1.85. 1.58	128	−0.9	0.1	0.7

[$(PPh_3)_2$Rh(closo-$CB_{11}H_{12}$)] [7], [$Cp(CO)_3$Mo(closo-$CB_{11}H_{12}$)] [24], [$Ag(PPh_3)_n$(closo-$CB_{11}H_{12}$)] ($n = 1, 2$) [25], [(cod)Rh(closo-$CB_{11}H_{12}$)] [9]. All measured in CD_2Cl_2 or $CDCl_3$ solutions.

[a] δ (^{1}H) CH for uncoordinated [closo-$CB_{11}H_{12}$] = 2.20 ppm.

[b] Numbers in parenthesis indicate J(RhP) in precursor diene complex.

[c] Antipodal vertex in italics.

[d] Chemical shift change from uncoordinated [closo-$CB_{11}H_{12}]^-$ [δ −7.3, −13.6, 16.4 ppm].

[e] BH obscured by cyclohexyl resonances between δ 1.0 and 2.0 ppm.

0.3–0.4 ppm. This is perhaps best demonstrated in the complex $[(PPh_3)_2Ag(closo\text{-}CB_{11}H_{12})]$ which only forms very loosely associated interactions between the metal and the cage [$\Delta\delta^{11}$B is small] and the chemical shift for the cage CH is more like uncoordinated $[closo\text{-}CB_{11}H_{12}]^-$ [δ 2.20 ppm].

5. Summary

Three new examples of *exo*-closo-rhodacarboranes have been synthesised in which the rhodium-phosphine fragments interact with the $[closo\text{-}CB_{11}H_{12}]$ anion through two 3 centre-2 electron bonds. The most reliable spectroscopic markers for this interaction, irrespective of the metal fragment, are an upfield shift in the ^{11}B-NMR spectrum and a small downfield shift of the CH proton in the ^{1}H-NMR spectrum. High-field proton shifts and reduced J(BH) coupling are also indicative of metal coordination, but their absence do not preclude M–H–B interactions. DFT calculations on model complexes show only a small energy difference between 7,12 and 7,8 coordination isomers, which suggests that both are accessible in solution and the solid-state (as is observed for PPh_3 and PCy_3 congeners, respectively).

6. Supplementary material

Crystallographic data (excluding structure factors) for the structural analysis have been deposited with the Cambridge Crystallographic Data Centre, CCDC no. 20430. Copies of this information may be obtained free of charge from The Director, CCDC, 12 Union Road, Cambridge CB2 1EZ, UK (Fax: +44-1223-336033; e-mail: deposit@ccdc.cam.ac.uk or www: http://www.ccdc.cam.ac.uk).

Acknowledgements

The Royal Society (ASW) and the EPSRC (AR) are thanked for funding. Johnson Matthey are thanked for the loan of precious metals. Dr. Nathan Patmore is also thanked for useful discussions.

References

[1] (a) R.T. Baker, M.S. Delaney, I.R.E. King, C.B. Knobler, J.A. Long, T.B. Marder, T.E. Paxson, R.G. Teller, M.F. Hawthorne, J. Am. Chem. Soc. 106 (1984) 2965;
(b) P.E. Behnken, J.A. Belmont, D.C. Busby, M.S. Delaney, I.R.E. King, C.W. Kreimendahl, T.B. Marder, J.J. Wilczynski, M.F. Hawthorne, J. Am. Chem. Soc. 106 (1984) 3011;
(c) C.B. Knobler, T.B. Marder, E.A. Mizusawa, R.G. Teller, J.A. Long, P.E. Behnken, M.F. Hawthorne, J. Am. Chem. Soc. 106 (1984) 2990;
(d) J.A. Long, T.B. Marder, M.F. Hawthorne, J. Am. Chem. Soc. 106 (1984) 3004.
[2] J.A. Long, T.B. Marder, P.E. Behnken, M.F. Hawthorne, J. Am. Chem. Soc. 106 (1984) 2979.
[3] J.A. Belmont, J. Soto, R.E. King, III, A.J. Donaldson, J.D. Hewes, M.F. Hawthorne, J. Am. Chem. Soc. 111 (1989) 7475.
[4] H. Yan, A.M. Beatty, T.P. Fehlner, Organometallics 21 (2002) 5029.
[5] (a) F. Teixidor, M.A. Flores, C. Viñas, R. Kivekäs, R. Sillanpää, Angew. Chem. Int. Ed. Engl. 35 (1996) 2251;
(b) F. Teixidor, M.A. Flores, C. Viñas, R. Kivekäs, R. Sillanpää, Organometallics 17 (1998) 4675;
(c) C. Viñas, M.A. Flores, R. Núñez, F. Teixidor, R. Kivekäs, R. Sillanpää, Organometallics 17 (1998) 2278;
(d) F. Teixidor, M.A. Flores, C. Viñas, R. Sillanpää, R. Kivekäs, J. Am. Chem. Soc. 122 (2000) 1963.
[6] F. Teixidor, R. Núñez, M.A. Flores, A. Demonceau, C. Viñas, J. Organomet. Chem. 614–615 (2000) 48.
[7] A. Rifat, N.J. Patmore, M.F. Mahon, A.S. Weller, Organometallics 21 (2002) 2856.
[8] C.A. Reed, Acc. Chem. Res. 31 (1998) 133.
[9] A.S. Weller, M.F. Mahon, J.W. Steed, J. Organomet. Chem. 614–615 (2000) 113.
[10] K. Shelly, D.C. Finster, Y.J. Lee, W.R. Scheidt, C.A. Reed, J. Am. Chem. Soc. 107 (1985) 5955.
[11] G.M. Sheldrick, SHELX-97, A Computer Program for Refinement of Crystal Structures, University of Göttingen, Germany.
[12] M.F. Guest, J.H. v. Lenthe, J. Kendrick, K. Schoffel, P. Sherwood, R.D. Amos, R.J. Buenker, H.J.J. v. Dam, M. Dupuis, N.C. Handy, I.H. Hillier, P.J. Knowles, V. Bonacic-Koutecky, W. v. Niessen, R.J. Harrison, A.P. Rendell, V.R. Saunders, A.J. Stone, A.H. d. Vries, GAMESS, Vol. 1, NRCC Software Catalogue, 1980.
[13] (a) A.D. Becke, J. Chem. Phys. 98 (1993) 5648;
(b) C. Lee, W. Yang, R.G. Parr, Phys. Rev. B 37 (1998) 785.
[14] (a) N. Godbout, D.R. Salahub, J. Andzelm, E. Wimmer, Can. J. Chem. 70 (1992) 560;
(b) N. Godbout, PhD, Université de Montréal, 1996.
[15] R.R. Schrock, J.A. Osborn, J. Am. Chem. Soc. 98 (1976) 2134.
[16] M.A. Fox, M.F. Mahon, N.J. Patmore, A.S. Weller, Inorg. Chem. 41 (2002) 4567.
[17] M.A. Esteruelas, F.J. Lahoz, E. Oñate, L.A. Oro, L. Rodrîguez, P. Steinert, H. Werner, Organometallics 15 (1996) 3436.
[18] M.H. Chisholm, J.C. Huffman, S.S. Iyer, J. Chem. Soc. Dalton Trans. (2000) 1483.
[19] D.J. Crowther, S.L. Borkowsky, D. Swenson, T.Y. Meyer, R.F. Jordan, Organometallics 12 (1993) 2897.
[20] G.S. Mhinzi, S.A. Litster, A.D. Redhouse, J.L. Spencer, J. Chem. Soc. Dalton Trans. (1991) 2769.
[21] K. Shelly, C.A. Reed, Y.J. Lee, W.R. Scheidt, J. Am. Chem. Soc. 108 (1986) 3117.
[22] T. Jelinek, P. Baldwin, W.R. Scheidt, C.A. Reed, Inorg. Chem. 32 (1993) 1982.
[23] S.V. Ivanov, J.J. Rockwell, S.M. Miller, O.P. Anderson, K.A. Solntsev, S.H. Strauss, Inorg. Chem. 35 (1996) 7882.
[24] N.J. Patmore, M.F. Mahon, J.W. Steed, A.S. Weller, J. Chem. Soc. Dalton Trans. (2001) 277.
[25] N.J. Patmore, C. Hague, J.H. Cotgreave, M.F. Mahon, C.G. Frost, A.S. Weller, Chem. Eur. J. 8 (2002) 2088.
[26] D.P. Fairlie, B. Bosnich, Organometallics 7 (1988) 936.
[27] J. Halpern, D.P. Riley, A.S.C. Chan, J.J. Pluth, J. Am. Chem. Soc. 99 (1977) 8055.
[28] S. Hermánek, Chem. Rev. 92 (1992) 325.